An exponentially weighted moving average control chart based on signed ranks for finite horizon processes

Theodoros Perdikis, Giovanni Celano, Stelios Psarakis, Philippe Castagliola

▶ **To cite this version:**

Theodoros Perdikis, Giovanni Celano, Stelios Psarakis, Philippe Castagliola. An exponentially weighted moving average control chart based on signed ranks for finite horizon processes. Quality Engineering, 2023, 35 (2), pp.290-303. 10.1080/08982112.2022.2125815 . hal-04061753

HAL Id: hal-04061753
https://hal.science/hal-04061753

Submitted on 7 Apr 2023

HAL is a multi-disciplinary open access archive for the deposit and dissemination of scientific research documents, whether they are published or not. The documents may come from teaching and research institutions in France or abroad, or from public or private research centers.

L'archive ouverte pluridisciplinaire **HAL**, est destinée au dépôt et à la diffusion de documents scientifiques de niveau recherche, publiés ou non, émanant des établissements d'enseignement et de recherche français ou étrangers, des laboratoires publics ou privés.

An Exponentially Weighted Moving Average Control Chart Based on Signed Ranks for Finite Horizon Processes

Theodoros Perdikis[a] and Giovanni Celano [b] and Stelios Psarakis [a]and Philippe Castagliola [c]

[a]Department of Statistics & Laboratory of Statistical Methodology, Athens University of Economics and Business Athens, Greece; [b]Università di Catania, Catania, Italy;[c]Nantes Université & LS2N UMR CNRS 6004, Nantes, France

ARTICLE HISTORY

Compiled September 2, 2022

Abstract

Distribution-free control charts are an efficient quality monitoring tool to inspect lots of parts manufactured within a finite production horizon. In this work, the performance of the Exponentially Weighted Moving Average chart based on the Wilcoxon signed rank statistic is investigated for on-line monitoring of finite production runs. The chart's on-target performance is evaluated through a specific non-homogeneous Markov chain model under different process scenarios. A numerical analysis is conducted for determining its optimal design and a performance comparison with other available schemes is presented for different symmetric distributions of observations. Finally, an illustrative example is presented to show a practical implementation of the investigated chart.

Keywords:Quality control; Statistical Process Monitoring; Markov processes; Distribution-free; Wilcoxon signed rank statistic.

1. Introduction

Statistical process monitoring (SPM), through the use of control charts, is widely implemented in industries as an efficient tool for the on-line monitoring of a product's characteristic of interest. The design of conventional control charts such as the Shewhart-type (see Shewhart (1939)), the EWMA (Exponentially Weighted Moving Average, see Roberts (1958)) or the CUSUM (Cumulative Sum, see Page (1954)) control charts is generally tackled by assuming on-line monitoring of long run processes. In particular, the chart's statistical design relies on the assumption that the process either never stops or it does after a very large number, say hundreds or thou-

CONTACT Stelios Psarakis. Email:psarakis@aueb.gr

sands, of inspections scheduled during the production horizon. However, in practice, in several manufacturing industries, process flexibility allows consecutive productions of lots of different part codes to be produced within a very short production horizon. For example, production of customized parts with the recent advanced manufacturing technologies, e.g. additive manufacturing based on 3D printing machines, is limited to delivering a finite number of parts within a short time horizon. Quality practitioners are required to monitor production by collecting a small number of samples and the main objective of monitoring is checking if the process location and/or dispersion is centered on a target value or not. At the end of each production run, the process resources are restored and reconfigured by performing proper set-up activities to begin manufacturing of the next scheduled lot of part codes. Frequently, in this manufacturing scenario only a few tens of inspections can be scheduled by quality practitioners for each production lot. As a result, a stream of SPM research has been developed on the design of control charts under the so called *Finite Horizon Process* (FHP) framework, see Chakraborti et al. (2021).

When a control chart should be selected to run in a FHP quality practitioners need to consider the following challenges:

- Under the FHP framework it is assumed that a finite lot of N parts is produced during a production horizon of finite length equal to H time units. To monitor the quality characteristic of interest, practitioners can schedule only I inspections during the production horizon H. Then, the sampling frequency between two consecutive inspections is defined as $h_0 = \frac{H}{I}$ time units. At each inspection, a sample of size n from a sub-population of $N_h = \frac{N}{I}$ parts is collected to run a control chart. The value of I could be restricted to a few tens due to constraints on the lot size and/or the rate of inspection.
- It should be noted that, due to the fact that the process setup frequently switches to a new part code, the underlying distribution of the quality characteristic to be monitored is not known: very often, the number of scheduled inspections is too small to allow this distribution to be identified. As a result, the use of distribution-free schemes is necessary (Chakrabortiand Graham (2019)).
- Usually, in productions where a large number of inspections is scheduled, the chart's statistical design is determined by its average run length properties, ARL = E(RL), where the run length (RL) is the random variable defined as " the count of points plotted on the control chart". However, these metrics are valid under the assumption that an infinite number of inspections is available. On the other hand, under the FHP framework, only a small number of inspections can be scheduled by the end of the production horizon. As a result, the distribution of the RL is truncated by the end of the production run. Therefore, different performance metrics have to be considered to design the control chart and evaluate its statistical performance.

As a consequence, with all being said, it is worth of interest to investigate the performance of conventional schemes (parametric or not), originally designed for long runs, under the FHP framework and to provide practitioners with guidelines about their design and statistical performance.
Many researchers have investigated the performance of control charts monitoring FHP. Under the assumption of normal observations, there are many contributions for monitoring shifts in the process mean (see, Nenes and Tagaras (2010), Castagliola et al. (2013), Nenes et al. (2014), Nenes et al. (2017)). Similarly, many nonparametric control charts have been widely investigated in literature under the FHP framework. For instance, there are many publications focusing on Shewhart control charts monitoring process location, which are based on distribution-free statistics such as the Sign control chart (Celano et al. (2016), Celano and Castagliola (2018)), the Wilcoxon signed rank control chart (Celano et al. (2016)) or the Mann-Whitney control chart (Celano et al. (2021)). Additionally, Bayesian control charts are another type of control schemes that can efficiently monitor shifts in the process location or scale in a FHP framework. In particular, at each inspection these charts allow the design parameters to be varied adaptively, based on prior knowledge and observed outcomes, see **?**, Wang and Lee (2015), Nikolaidis and Tagaras (2017).

In this work, we aim to investigate the performance of the EWMA control chart based on the Wilcoxon signed rank statistic introduced by Graham et al. (2011) under the FHP framework. With this control chart, the location deviation of the process from a nominal target value specified by the quality practitioner can be monitored for observations having a symmetric distribution.

The remainder of this work is organised as follows. In Section 2, the operation and design of the EWMA chart based on the Wilcoxon signed rank statistic is presented. Furthermore, its statistical design under the FHP framework is introduced and appropriate metrics are discussed regarding the determination of its performance. In Section 3, a numerical analysis is conducted on the selection of its design parameters and their effect on the investigated control chart's performance. In Section 4, the performance of the proposed chart is compared with existing nonparametric schemes under different process scenarios. Finally, in Section 5 an illustrative example is presented to show a practical implementation of the proposed scheme, while in Section 6 some concluding remarks and suggestions for future works are discussed.

2. Implementation of the EWMA chart based on Signed Ranks for FHP

The nonparametric EMWA chart based on the Wilcoxon signed rank statistic has been originally introduced by Graham et al. (2011) for long run processes. In particular, its statistical performance has been investigated for several symmetric distributions

under the assumption that the process operates *indefinitely*. Therefore, its statistical design and implementation were entirely based on the fact that the process theoretically never stops, meaning that practitioners have at their disposal thousands of potential inspections. Under the FHP framework, this assumption does no longer hold and the effect of varying control limits for the EWMA control chart must be investigated by calculating proper performance metrics defined for a FHP. In this work, we aim to revisit the EWMA control chart based on Wilcoxon signed rank statistic by providing practitioners with detailed guidelines about its design, performance and implementation under the FHP framework.

2.1. *Implementation in a FHP*

Suppose that, at each scheduled inspection $i = 1, 2, \ldots, I$ during the production run, a subgroup of observations $\{X_{i,1}, X_{i,2}, \ldots, X_{i,n}\}$ having size n is collected from a subpopulation having size N_h. We assume that the observations $X_{i,j}$, for $i = 1, \ldots I$, $j = 1, \ldots n$ are i.i.d. random variables with unknown continuous symmetric distribution. Without loss of generality, we also assume that N_h is an even number, as in Celano et al. (2016), and θ_t denotes the process median, which is the location parameter of interest at time $t = h_0, 2 \times h_0, \ldots, H$. In general, during the production run the process median is equal to

$$\theta_t = \begin{cases} \theta_0, & t = h_0, 2 \times h_0, \ldots, (i-1) \times h_0 \\ \theta_1, & t = i \times h_0, (i+1) \times h_0, \ldots, H \end{cases},$$

where $\theta_1 = \theta_0 + \delta\sigma$, δ is the shift magnitude and $i-1$ is the inspection index immediately before the shift. Similarly to what was suggested by Zimmer et al. (2000) for long run processes, different operating conditions can be considered for the process finite production horizon:
- *on-target* condition: the process starts and remains on-target ($\theta_t = \theta_0$ for $t = h_0, 2 \times h_0, \ldots, H$) without any location shift during the production run. In this case, the control chart should not signal any alarm. Any signal triggering is a false alarm;
- *off-target* condition: the process starts off-target ($\theta_t = \theta_1$ for $t = h_0, 2 \times h_0, \ldots$) due to an imperfect set-up. The location shift is conventionally assumed immediately after the start of the production run. In this case, all I scheduled inspections are available to the control chart to trigger a signal by the end of the production run.
- *on-to-off-target* condition: the process starts on-target ($\theta_t = \theta_0$ for $t = h_0, 2 \times h_0, \ldots, (i-1) \times h_0$) with a location shift occurring during the production run before inspection i. In this case, only $I - i + 1$ scheduled inspections are available to the control chart to trigger a signal by the end of the production run.

At each inspection i, the Wilcoxon signed rank statistic (SR_i) from sample i of observations is computed as follows:

$$\mathrm{SR}_i = \sum_{j=1}^{n} \mathrm{sign}(X_{i,j} - \theta_0) L_{i,j}, \tag{1}$$

where $\mathrm{sign}(X_{i,j} - \theta_0) = -1, 0$ or 1, if $X_{i,j} < \theta_0$,$X_{i,j} = \theta_0$ or $X_{i,j} > \theta_0$, respectively. Additionally, $L_{i,j} \in \{1, 2, \ldots, n\}$ denotes the rank of the absolute value of the differences $|X_{i,j} - \theta_0|, j = 1, 2, ..., n$, for inspection $i = 1, 2, \ldots, I$. It is worth stretching that, due to the assumption that each sample follows a continuous distribution, the condition $X_{i,j} = \theta_0$, corresponding to an observation tied to the target median is very unlikely to occur. For the computation of the sign statistic, Castagliola et al. (2020) provide some practical solutions to the problem of tied observations that can be easily adapted to the WSR statistic.

Generally, the SR_i statistic presented in (1) can be alternatively expressed as:

$$\mathrm{SR}_i = 2\mathrm{SR}_i^+ - \frac{n(n+1)}{2}, \tag{2}$$

where SR_i^+ is the sum of positive signed ranks and is often called as the *null* Wilcoxon distribution. Moreover, by definition, the SR_i statistic is defined on $\{-\frac{n(n+1)}{2}, -\frac{n(n+1)}{2} + 2, \ldots, \frac{n(n+1)}{2} - 2, \frac{n(n+1)}{2}\}$. A simple and efficient way to compute the distribution of SR_i is through the *null* Wilcoxon distribution, SR_i^+ using the relation presented in (2), see Gibbons and Chakraborti (20121).

Finally, at each inspection i, the charting statistic of the two-sided EWMA chart based on signed ranks (WSR EWMA chart) is defined by the following recursive formula:

$$Z_i = \lambda \times \mathrm{SR}_i + (1 - \lambda) Z_{i-1}, \tag{3}$$

where $Z_0 = \mathrm{E}_0(\mathrm{SR}_i)$ and $\mathrm{E}_0(\mathrm{SR}_i)$ is the on-target mean of SR_i. Considering a finite horizon process for which the number of inspections is small (say $I < 50$), the *time-varying* (TV) control limits of the proposed chart under the FHP framework are equal to:

$$\mathrm{UCL}(i) = \mathrm{E}_0(\mathrm{SR}_i) + K\sqrt{\mathrm{V}_0(\mathrm{SR}_i)\frac{\lambda}{(2-\lambda)}(1-(1-\lambda)^{2i})}$$

$$\mathrm{LCL}(i) = \mathrm{E}_0(\mathrm{SR}_i) - K\sqrt{\mathrm{V}_0(\mathrm{SR}_i)\frac{\lambda}{(2-\lambda)}(1-(1-\lambda)^{2i})}$$

When the process is on-target the mean and variance of SR_i are equal to (Graham et

al. (2011)):

$$\begin{aligned} \mathrm{E}_0(\mathrm{SR}_i) &= 0, \\ \mathrm{V}_0(\mathrm{SR}_i) &= \frac{n(n+1)(2n+1)}{6}. \end{aligned}$$

Additionally, for a sufficiently large number of I inspections, the above limits converge to the *asymptotic* (A_∞) control limits defined as

$$\mathrm{UCL}_\infty = \mathrm{E}_0(\mathrm{SR}_i) + K\sqrt{\mathrm{V}_0(\mathrm{SR}_i)\frac{\lambda}{(2-\lambda)}}$$

$$\mathrm{LCL}_\infty = \mathrm{E}_0(\mathrm{SR}_i) - K\sqrt{\mathrm{V}_0(\mathrm{SR}_i)\frac{\lambda}{(2-\lambda)}}$$

It is worth remembering that for a finite horizon process the control limits rarely converge to their asymptotic values due to the small values of I. For this reason, we discourage practitioners from implementing the EWMA control chart with $(\mathrm{LCL}_\infty, \mathrm{UCL}_\infty)$ in a FHP. Later, in the Numerical Analysis Section we also prove that, as expected, the TV control limits boost the control chart's detection capability vs. the A_∞ control limits.

2.2. *Selection of design parameters*

Generally, the design and performance of conventional EWMA charts for long-run processes are derived through their RL (Run Length) distribution. In particular, the most commonly used metric for the charts' performance is the ARL (Average Run Length), defined as "the expected number of plotted points until the first signal is triggered by the control chart" (out-of-control state) or as "the expected number of plotted points between two successive false alarms" (in-control state). However, under the FHP framework, this metric is inefficient due to the fact that its operation assumes that $I \to \infty$. In this work, the chart's operation and statistical design will be derived though the following metrics (Celano and Castagliola (2018)):

- Let us assume that the process is on-target. The chart's design parameters (λ, K) are selected by considering the FAP (False Alarm Probability) metric: it is defined as the probability of at least one false alarm occurring by the end of the production run, given a finite number of I scheduled inspections. The design parameters (λ, K) of the EWMA control chart are selected by fixing at a nominal value FAP_0 the expected probability of false alarm during the production run. For the computation of the FAP value, a discrete Markov chain approach origi-

nally introduced by Brook and Evans (1972) for long run processes is adapted to FHP. A detailed presentation regarding the computation of FAP is provided in the Appendix A.

- The chart's off-target statistical performance is determined through the $\mathrm{SP}(i, g)$ (signal probability) defined as "the probability to get from the control chart a true signal *by* the g-th inspection *after* the event shifting the process location, assumed to occur *before* inspection i". In particular, assuming that the assignable cause occurs before the i-th inspection, the signal probabilities $\mathrm{SP}(i, g)$ are calculated as follows:

$$\mathrm{SP}(i, g) = \sum_{k=1}^{g} \mathrm{P}(Z_k > \mathrm{UCL}(k) \text{ or } Z_k < \mathrm{LCL}(k) | \theta = \theta_1)$$

where $g \leq (I-i)+1$ denotes the g-th scheduled inspection after the occurrence of the assignable cause. For instance, assuming that a shift occurs before inspection $i = 1$ i.e. for an *off-target* process, then $g = \{1, 2, \ldots, I\}$. Therefore, when $g = 1$, $\mathrm{SP}(1, 1)$ denotes the probability that the control chart triggers a true off-target signal *by the first inspection* after the occurrence of the assignable cause; when $g = 3$, $\mathrm{SP}(1, 3)$ denotes the probability that the control chart triggers a true off-target signal by the third inspection after the occurence of the assignable cause; when $g = I$, $\mathrm{SP}(1, I)$ is the probability that the control chart triggers a true off-target signal *by the end of the production run.* Thus, given the process location shift, a plot of $\mathrm{SP}(i, g)$, can be generated. This plot is known as the signal probability profile, as defined by Celano et al. (2021). Finally, assuming that the process shifts to the off-target state before inspection i, an efficient metric to quantify the chart's overall statistical performance during a production run is the $\overline{\mathrm{SP}}(i)$ (Average Signal Probability), defined as:

$$\overline{\mathrm{SP}}(i) = \frac{1}{G_i} \sum_{g=1}^{G_i} \mathrm{SP}(i, g)$$

For the computation of every $\mathrm{SP}(i, g)$ profile, we consider a Monte Carlo simulation because considering the process change-point at any time during the production run condition does not allow the vector of initial probabilities to be defined for the Markov chain. Furthermore, a steady-state condition cannot be assumed within a few inspections. Neither the zero state nor the FIR feature can be considered, because they would assume either an on-target or an off-target process. Therefore, we have decided to simulate N_{sim} runs, for each process location change-point during the production run to overcome the problem and to perform the study. We considered $N_{sim} = 10^6$ simulation runs to get reliable estimates of the off-target WSR EWMA chart's performance. It should be clarified the fact that, even though the chart's off-target performance is determined through a simulation-based method, the obtained results are not affected

by the selected number of simulation runs, (see Appendix B).

3. Numerical analysis

The proper determination of the parameters (λ, K) is essential to design an efficient EWMA chart. In particular, the couple of design parameters (λ, K) should be obtained under the condition that the corresponding FAP metric is equal to a nominal value FAP_0. The correct estimation of FAP values can be affected by the number of subintervals S chosen for the Markov chain, see Appendix A. Thus, a preliminary study has been performed on the correct tuning of the Markov chain. In Figure 1, several plots present FAP values as a function of the number of Markov chain's subintervals $S = \{251, 301, \ldots, 1001\}$ for $(I = 20, N_h = 200)$ and $n \in \{5, 10, 15, 20\}$ using the A_∞ control limits. Additionally, for each case, an error bandwidth $\text{FAP}^{S=1001} \pm 3\%$ (dashed lines) is used where $\text{FAP}^{S=1001}$ (solid lines) represents the FAP value computed for $S = 1001$, (i.e a substantially large number of subintervals). Finally, the couple $(\lambda, K) = (0.2, 2.5)$ has been randomly selected only for illustration purposes. From Figure 1 we may conclude that the FAP values are inside the error bandwidth and, as n increases, they become steady around the value $\text{FAP}^{S=1001}$. Looking at the plots in Figure 1, setting $S \approx 501$ can be considered as a reasonable choice regarding the number of subintervals.

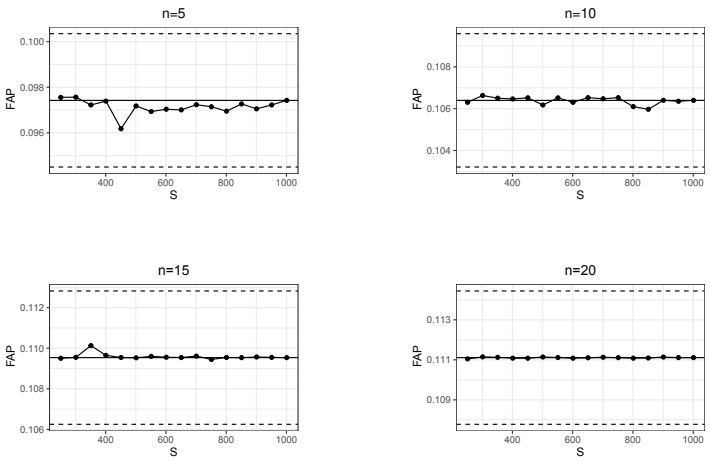

Figure 1. FAP values vs. the number of subintervals S for $(I = 20, N_h = 200)$, $(\lambda, K) = (0.2, 2.5)$ and $n \in \{5, 10, 15, 20\}$

3.1. *On-target and off-target performance*

Similarly to any distribution-free control chart, our proposed scheme can be designed without any assumption about the underlying distribution of observations. In particular, for a given process scenario (n, N_h, I), practitioners want to select a couple of design parameters (λ, K) that meets the constraint on false alarm probability $\text{FAP} = \text{FAP}_0$, (*on-target* performance study). In particular, it should be mentioned that, for a distribution-free control chart, due to the discrete nature of the statistic to

Table 1. Values of K when $I \in (10, 20)$, $\text{FAP}_0 \in \{0.01, 0.1\}$ under different process scenarios (n, N_h, I)

$\text{FAP}_0 = 0.01$

		$I \in (10,20)$				
		λ				
N_h	n	0.05	0.1	0.15	0.2	0.25
50	5	(2.67,2.85)	(2.761,3.019)	(2.832,3.098)	(2.873,3.127)	(2.893,3.126)
	10	(2.69,2.86)	(2.791,3.06)	(2.88,3.148)	(2.941,3.209)	(2.98,3.217)
	15	(2.69,2.87)	(2.8,3.07)	(2.891,3.181)	(2.961,3.241)	(3.01,3.263)

$\text{FAP}_0 = 0.1$

		$I \in (10,20)$				
		λ				
N_h	n	0.05	0.1	0.15	0.2	0.25
150	5	(1.88,2.07)	(2.011,2.298)	(2.11,2.419)	(2.199,2.489)	(2.25,2.518)
	10	(1.88,2.08)	(2.02,2.302)	(2.128,2.443)	(2.219,2.523)	(2.278,2.57)
	15	(1.88,2.079)	(2.02,2.31)	(2.129,2.451)	(2.227,2.532)	(2.287,2.581)

be monitored (such as the Sign or the Wilcoxon statistics), it is not always possible to find design parameters to get exactly $\text{FAP} = \text{FAP}_0$, see Graham et al. (2011). As a result, for a given process scenario (n, N_h, I), couples (λ, K) can be selected if:

$$|\text{FAP} - \text{FAP}_0| \leq \tau$$

where τ is a fixed constant. Without loss of generality, we set $\tau = 0.001$. In Table 1 several couples of the design parameters (λ, K) are reported for the WSR EWMA control chart under different process scenarios (n, N_h, I). In particular, for a given value of $\lambda \in \{0.01, 0.025, 0.05, 0.1, 0.2\}$ and $\text{FAP}_0 \in \{0.01, 0.1\}$, the corresponding values of K have been computed for a population size $N_h \in \{50, 150\}$ between two consecutive inspections, sample size $n \in \{5, 10, 15\}$ and the scheduled number of inspections is $I \in \{10, 20\}$. In general, in conventional EWMA schemes, as λ increases the corresponding value of K also increases. From Table 1, it may be concluded that this trend is also valid for the proposed chart implemented in the FHP scenario. In particular, for the process scenario $(n, N_h, I, \text{FAP}_0)$=$(5, 50, 10, 0.01)$ we may see that for $\lambda \in \{0.05, 0.1, 0.15, 0.2, 0.25\}$ we get $K \in \{2.67, 2.761, 2.832, 2.873, 2.893\}$.

The off-target performance of the WSR EWMA chart is examined under the following symmetric distributions of observations:

- normal distribution, $\text{N}(0, 1)$
- Student t distribution, $t(8)$
- logistic distribution, $L\left(0, \frac{\sqrt{3}}{\pi}\right)$
- contaminated normal distribution $CN(0.05, 2)$

where the location and scale parameters for each distribution have been chosen in order to have zero mean and unit variance.

Before we proceed to any conclusions or performance evaluations for the WSR EMWA control chart in the FHP scenario, for the sake of completeness it is important to investigate the effect of the two types of control limits (i.e. the TV and A_∞ control limits), described at the beginning of this Section, on the chart's best off-target performance. Under the design of a conventional WSR EMWA chart for long runs, due to the availability of a very large number of inspections the chart's control limits become steady and so the A_∞ limits can be used. On the other hand, under FHP, only a few inspections are available by the end of the production. As a consequence, the "steady" control limits cannot be achieved and the use of the TV limits is crucial. In Figure 2, assuming the $N(0,1)$ distribution, for $\delta \in \{0.25, 0.5, 0.75, 1\}$ the corresponding probability profiles $SP(1,g)$ of the WSR EWMA chart are presented using the A_∞, and TV control limits, considering the process scenario $(I, n, N_h) = (10, 10, 100)$. Moreover, setting $\lambda = 0.05$, we get $K = 2.69$ (using A_∞ limits) and $K = 2.17$ (using the TV limits). Finally, the design parameters (λ, K) have been chosen in order to get that FAP ≈ 0.01. From Figure 2, it can be clearly seen that using the TV control limits the signal probabilities are significantly higher than for the A_∞ limits. As an immediate consequence, under the FHP framework the use of TV limits significantly increases the chart's detection power for any shift magnitude in the process median. This is an expected finding since the number of scheduled inspections is small and the narrower TV limits at the beginning of the process allow a faster detection speed than the wider A_∞ limits.

In Table 2, for each distribution listed above, the corresponding off-target performance for the WSR EWMA chart with TV limits is presented, considering the process scenario $(n, N_h, I, \text{FAP}_0)$=$(10, 150, 10, 0.1)$ for $\lambda \in \{0.05, 0.1, 0.2\}$ in terms of the $\overline{SP}(1)$ metric for an *off-target* process. For each case, as expected, we may observe that as δ increases $\overline{SP}(1) \to 1$. Values of $\overline{SP}(1)$ close to one mean that the WSR EWMA control chart immediately signals the process location shift from the target since the first scheduled inspection. For instance, when the underlying distribution is $N(0,1)$ for $\lambda = 0.05$ and $\delta \in \{0.25, 0.5, 0.75, 1.25, 1.5, 2\}$, the corresponding values for the average signal probabilities are
$\overline{SP}(1) \in \{0.5348, 0.8548, 0.9475, 0.9947, 0.9989, 1\}$.

Table 2. Off-target performance in terms of $\overline{\text{SP}}(1)$ for the WSR EWMA chart with TV limits for $(n, N_h, I, \text{FAP}_0)$=$(10, 150, 10, 0.1)$ and $\lambda \in \{0.05, 0.1, 0.2\}$. *Off-target* process scenario, $i = 1$.

	N(0, 1)			$t(8)$		
δ	$\lambda = 0.05$	$\lambda = 0.1$	$\lambda = 0.2$	$\lambda = 0.05$	$\lambda = 0.1$	$\lambda = 0.2$
0.25	0.5348	0.4835	0.4118	0.5702	0.5202	0.4502
0.5	0.8548	0.8270	0.7874	0.8725	0.8471	0.8117
0.75	0.9475	0.9313	0.9097	0.9538	0.9390	0.9195
1.25	0.9947	0.9902	0.9816	0.9941	0.9894	0.9820
1.5	0.9989	0.9974	0.9937	0.9981	0.9960	0.9922
2	1.0000	0.9999	0.9997	0.9998	0.9994	0.9987

	$L\left(0, \frac{\sqrt{3}}{\pi}\right)$			$CN(0.05, 2)$		
δ	$\lambda = 0.05$	$\lambda = 0.1$	$\lambda = 0.2$	$\lambda = 0.05$	$\lambda = 0.1$	$\lambda = 0.2$
0.25	0.5724	0.5222	0.4524	0.5508	0.4999	0.4282
0.5	0.8732	0.8478	0.8129	0.8645	0.8377	0.8005
0.75	0.9538	0.9389	0.9197	0.9524	0.9369	0.9162
1.25	0.9940	0.9891	0.9816	0.9959	0.9919	0.9843
1.5	0.9981	0.9959	0.9920	0.9992	0.9981	0.9950
2	0.9998	0.9995	0.9988	1.0000	1.0000	0.9998

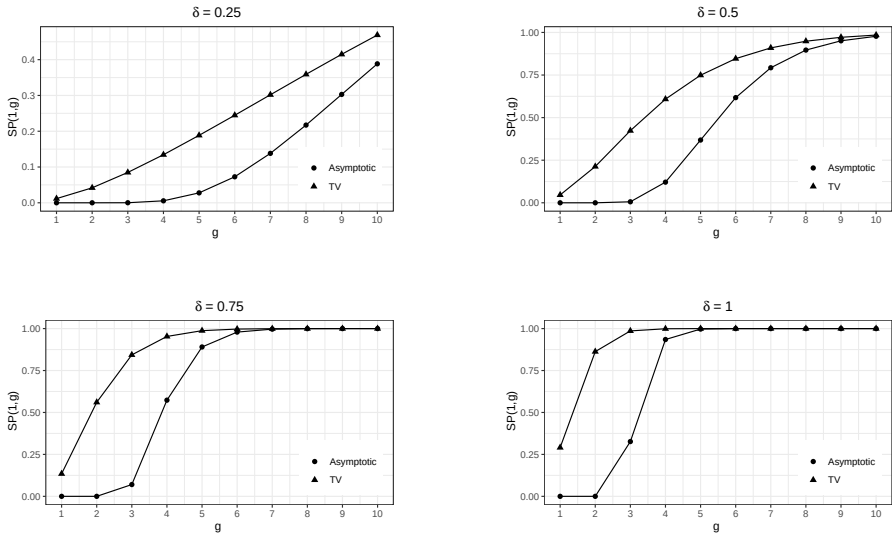

Figure 2. $\text{SP}(1, g)$ values (*off-target* process) using A_∞ and TV control limits vs. g for $n = 10$, when $(I, N_h) = (10, 100)$ and $\delta \in \{0.25, 0.5, 0.75, 1\}$ under $\text{N}(0, 1)$

To show the effect of λ on the chart's off-target performance, Figure 3 plots the $\overline{\text{SP}}(1)$ values presented in Table 2. Within each plot, each dotted line represents the off-target performance of the WSR EWMA chart for $\lambda \in \{0.05, 0.1, 0.2\}$. It can be seen that, for small to moderate shifts, the corresponding $\overline{\text{SP}}(1)$ values are maximized by setting $\lambda = 0.05$. On the other hand, as δ increases, the probabilities tend to be the same regardless the value of λ. As a result, choosing $\lambda = 0.05$ can be considered as a reasonable choice.

Similarly, it is important to investigate the effect of the sample size n on the off-target performance of the WSR EWMA chart under the FHP framework. In general, as the sample size increases the chart's shift detection ability is significantly improved. However, in real-life applications, quality practitioners may not have at their disposal a large set of observations at each inspection. In Figure 4, the $\overline{\text{SP}}(1)$ values using TV control limits are reported, under different process scenarios for small to moderate sample sizes $n \in \{1, 5, 10, 15\}$. From Figure 4 it can be seen that, as the sample size becomes larger, the $\overline{\text{SP}}(1)$ values increase. In particular, for small shifts ($\delta = 0.5$), when $n = 1$ we obtain $\overline{\text{SP}}(1) < 0.1$ (FAP $= 0.01$) and $\overline{\text{SP}}(1) = 0.14$ ($\text{FAP}_0 = 0.1$). On the other hand, when $n = 15$ we obtain $\overline{\text{SP}}(1) \approx 0.8$ (FAP $= 0.01$) and $\overline{\text{SP}}(1) \approx 0.91$ ($\text{FAP}_0 = 0.1$). For moderate to large shifts ($\delta > 1$) and $n > 10$ the corresponding $\overline{\text{SP}}(1)$ values tend to be the same. As consequence, it can be concluded that the use of moderate sample sizes ($n \approx 10$) yields to an efficient overall performance for detecting small to large shifts.

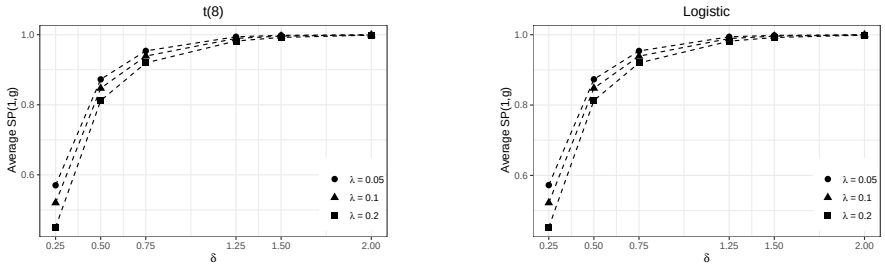

Figure 3. Effect of λ: $\overline{\text{SP}}(1)$ values using TV control limits considering the process scenario $(n, N_h, I, \text{FAP}_0)$=$(10, 150, 10, 0.1)$ for $\lambda \in \{0.05, 0.1, 0.2\}$ under the $t(8)$ (left) and the $L\left(0, \frac{\sqrt{3}}{\pi}\right)$ (right) distributions

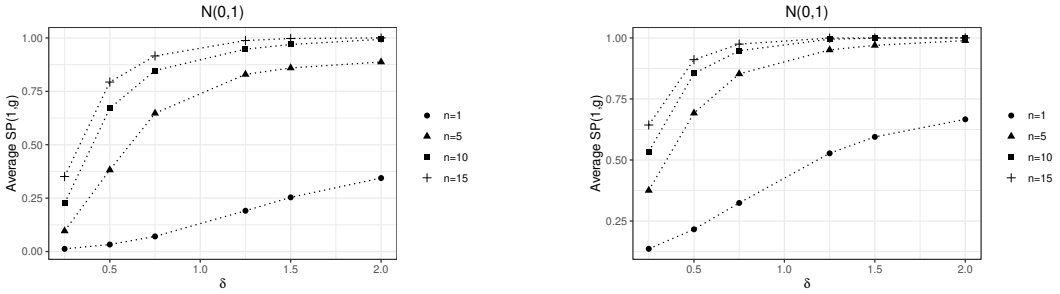

Figure 4. Effect of the sample size n: $\overline{\text{SP}}(1)$ values using TV control limits, when $(N_h, I, \text{FAP}_0) = (150, 10, 0.01)$ (left) and $(N_h, I, \text{FAP}_0) = (150, 10, 0.1)$ (right) for $\delta \in \{0.25, 0.5, 0.75, 1.25, 1.5, 2\}$ and $n \in \{1, 5, 10, 15\}$

It is worth noting that a location shift can occur at any time during the production run, (*on-to-off-target* process condition). In the numerical analysis presented so far, only for illustration purposes it has been assumed that an assignable cause occurs immediately

Table 3. SP(i,g) values assuming that an assignable cause occurs before inspection i under $N(0,1)$ for $(n=15, N_h=200, I=10, \text{FAP}_0=0.1)$ with TV limits. *On-to-off-target* scenario.

	$\delta=0.5$					$\delta=0.75$				
	$i=1$	$i=3$	$i=5$	$i=7$	$i=9$	$i=1$	$i=3$	$i=5$	$i=7$	$i=9$
	0.4440	-	-	-	-	0.7705	-	-	-	-
	0.7796	-	-	-	-	0.9787	-	-	-	-
	0.9219	0.1586	-	-	-	0.9985	0.2849	-	-	-
	0.9744	0.4777	-	-	-	0.9999	0.7899	-	-	-
SP(i,g)	0.9920	0.7544	0.1032	-	-	1	0.9738	0.1811	-	-
	0.9977	0.9050	0.3475	-	-	1	0.9980	0.6255	-	-
	0.9993	0.9676	0.6334	0.0796	-	1	0.9999	0.9221	0.1386	-
	0.9998	0.9899	0.8360	0.2815	-	1	1	0.9918	0.5225	-
	1	0.9971	0.9385	0.5539	0.0670	1	1	0.9994	0.8657	0.1165
	1	0.9992	0.9794	0.7789	0.2422	1	1	1	0.9813	0.4568

	$\delta=1$					$\delta=1.5$				
	$i=1$	$i=3$	$i=5$	$i=7$	$i=9$	$i=1$	$i=3$	$i=5$	$i=7$	$i=9$
	0.9469	-	-	-	-	0.9996	-	-	-	-
	0.9995	-	-	-	-	1	-	-	-	-
	1	0.4088	-	-	-	1	0.5614	-	-	-
	1	0.9446	-	-	-	1	0.9990	-	-	-
SP(i,g)	1	0.9993	0.2568	-	-	1	1	0.3478	-	-
	1	1	0.8176	-	-	1	1	0.9484	-	-
	1	1	0.9935	0.1963	-	1	1	1	0.2674	-
	1	1	0.9999	0.7123	-	1	1	1	0.8698	-
	1	1	1	0.9780	0.1636	1	1	1	0.9999	0.2235
	1	1	1	0.9997	0.6375	1	1	1	1	0.8023

after the production begins (i.e. for $i=1$, *off-target* condition). In order to investigate the control chart's signal probability profile for the *on-to-off-target* process condition, in Table 3 several scenarios are considered under $\text{N}(0,1)$ for $(n=15, N_h=200, I=10, \text{FAP}_0=0.1, i\in\{1,3,5,7,9\})$ using $(\lambda, K)=(0.05, 1.88)$. In particular, for $\delta=0.5$, when $i=9$, (i.e. we assume that the shift has occurred before inspection 9), the corresponding probabilities of detecting a shift *by* inspection $g=\{1,2\}$ *after* the occurrence of the shift, are $\text{SP}(i,g)=\{0.067, 0.24\}$. As expected, these probabilities are quite low, since the control chart should detect a small shift by only two available inspections. On the other hand, for $\delta=1.5$ and $i=9$ the corresponding probabilities are $\text{SP}(i,g)=\{0.2235, 0.8023\}$. For the other investigated cases $i\in\{3,5,7\}$ it is evident that the signal probabilities converge to 1 regardless of the shift magnitude.

4. Performance comparisons

In this Section we aim to investigate the performance of the WSR EWMA chart versus other nonparametric control charts under the FHP framework: in particular, we consider the Sign EWMA control chart with TV limits (Celano and Castagliola (2018)) and the Shewhart Wilcoxon Signed Rank control chart (Celano et al. (2016)). In Table 4, performances comparisons between the Sign and the WSR EWMA control charts are presented under different process scenarios $(n, N_h, I, \text{FAP}_0)$. In particular,

for each investigated distribution of observations, the percentage difference between the Sign and the WSR control charts is presented and computed as:

$$\Delta = \frac{\overline{\mathrm{SP}}(1)^{\mathrm{SR}} - \overline{\mathrm{SP}}(1)^{\mathrm{SN}}}{\overline{\mathrm{SP}}(1)^{\mathrm{SN}}} \times 100\% \tag{4}$$

where $\overline{\mathrm{SP}}(1)^{\mathrm{SR}}$ and $\overline{\mathrm{SP}}(1)^{\mathrm{SN}}$ are the corresponding average probabilities for the WSR and Sign EWMA charts, respectively. Additionally, for each scheme, setting $\lambda = 0.05$, the corresponding value of K has been computed for FAP $\in \{0, 01, 0.1\}$. It is clear that values of $\Delta > 0$ show the superiority of the WSR EWMA chart because they correspond to an higher average signal probability. From Table 4 we may conclude that for FAP $= 0.1$ the WSR outperforms the Sign EWMA chart except for large shifts with $n = 5$. On the other hand, for small to moderate shifts the WSR has a better performance, regardless of the sample size or the underlying distribution. Similarly, for FAP $= 0.01$, the WSR EWMA chart has a better performance for small to moderate shifts ($\delta < 1.25$). For $n > 15$ (large sample size) and $\delta > 1.25$ (large shifts) the Sign EWMA chart performs slightly better under the $t(8)$ and $L\left(0, \frac{\sqrt{3}}{\pi}\right)$ distributions. As a consequence, for small to moderate sample sizes and shift mangitudes the WSR EWMA chart outperforms the Sign EWMA control chart. It is worth stretching that these findings are consistent with the perfomance comparisons for long run processes performed by Graham et al. (2011) between these two schemes in terms of the ARL metric.

Table 5 shows values of Δ between the WSR EWMA chart and the WSR Shewhart control chart. Note that, in order to perform fair comparisons, the design of the EWMA chart is selected as to get the same FAP value as the Shewhart chart. In fact, it is well acknowledged that a main disadvantage of Shewhart distribution-free schemes is that frequently these charts cannot be designed to get a FAP exactly equal to the fixed nominal value FAP_0 (i.e. close to 0.01 or 0.1). Moreover, in Table 5, the coefficient C denotes the width of the control limits for the Shewhart control chart. From the results in Table 5 we may conclude that, for small shifts, the WSR EWMA chart has the best performance. On the other hand, for large shifts, the WSR Shewhart chart performs slightly better. In general, for large shifts and using a small value of λ in the EWMA chart, Shewhart-type schemes perform slightly better. Of course, by setting $\lambda \approx 0.2$ the EWMA chart will be superior for detecting large shifts. Nevertheless, in most cases, the differences are close to zero because the signal probabilities rapidly tend to one for both charts. As a consequence, both schemes can be considered for detecting large shifts in the process.

It should be noted that, for the performance comparisons performed above, it has been assumed that the shift occurs at the start of the process ($i = 1$, *off-target* condition). However, as it was highlighted in Section 3, a shift in a process can occur at any

Table 4. Performance comparisons in terms of $\overline{\text{SP}}(1)$ between the Sign and WSR EWMA charts for ($N_h = 150, I = 20$) with TV limits. *Off-target* process scenario, ($i = 1$).

$\text{FAP}_0 = 0.01$

	N(0, 1)				$t(8)$			
δ	$n = 5$	$n = 10$	$n = 15$	$n = 20$	$n = 5$	$n = 10$	$n = 15$	$n = 20$
0.25	**17.66**%	**23.43**%	**15.94**%	**10.46**%	**10.75**%	**14.18**%	**8.73**%	**4.94**
0.5	**12.56**%	**6.37**%	**3.32**%	**1.93**%	**6.7**%	**3.28**%	**1.45**%	**0.65**%
0.75	**4.18**%	**2.14**%	**0.86**%	**0.38**%	**2.04**%	**0.93**%	**0.1**%	-0.17%
1.25	**0.66**%	-1.1%	**0.02**%	**0.09**%	**0.2**%	-1.61%	-0.24%	-0.03%
1.5	**0.23**%	-2.39%	**0.06**%	**0.03**%	**0.03**%	-2.63%	-0.13%	0%
2	**0.01**%	-4.01%	**0.01**%	0%	-0.01%	-3.92%	-0.04%	0

	$L\left(0, \frac{\sqrt{3}}{\pi}\right)$				$CN(0.05, 2)$			
δ	$n = 5$	$n = 10$	$n = 15$	$n = 20$	$n = 5$	$n = 10$	$n = 15$	$n = 20$
0.25	**9.87**%	**12.41**%	**7.46**%	**3.8**%	**17.3**%	**23.18**%	**15.55**%	**9.87**
0.5	**5.76**%	**2.82**%	**1.22**%	**0.44**%	**11.47**%	**5.76**%	**3.05**%	**1.77**%
0.75	**1.78**%	**0.77**%	0%	-0.23%	**3.82**%	**1.93**%	**0.77**%	**0.33**%
1.25	**0.19**%	-1.6%	-0.25%	-0.04%	**0.56**%	-1.33%	**0.03**%	**0.08**%
1.5	**0.03**%	-2.59%	-0.13%	0%	**0.18**%	-2.6%	**0.07**%	**0.02** %
7	-0.01%	-3.89%	-0.02%	0 %	**0.01**%	-4.14%	**0.01**%	0%

$\text{FAP}_0 = 0.1$

	N(0, 1)				$t(8)$			
δ	$n = 5$	$n = 10$	$n = 15$	$n = 20$	$n = 5$	$n = 10$	$n = 15$	$n = 20$
0.25	**10.1**%	**13.09**%	**8.17**%	**6**%	**6.98**%	**8.59**%	**4.79**%	**3.5**%
0.5	**5.49**%	**4.32**%	**2.57**%	**1.91**%	**2.92**%	**2.87**%	**1.63**%	**1.17**%
0.75	**1.36**%	**2.26**%	**1.29**%	**0.87**%	**0.12**%	**1.59**%	**0.81**%	**0.52**%
1.25	-2.04%	**1.02**%	**0.27**%	**0.07**%	-2.55%	**0.71**%	**0.16**%	**0.03**%
1.5	-3.13%	**0.59**%	**0.07**%	**0.01**%	-3.42%	**0.4**%	**0.04**%	0%
2	-4.41%	**0.1**%	0%	0%	-4.37%	**0.09**%	0%	0

	$L\left(0, \frac{\sqrt{3}}{\pi}\right)$				$CN(0.05, 2)$			
δ	$n = 5$	$n = 10$	$n = 15$	$n = 20$	$n = 5$	$n = 10$	$n = 15$	$n = 20$
0.25	**6.23**%	**7.76**%	**4.36**%	**3**%	**10.3**%	**12.71**%	**7.93**%	**5.76**%
0.5	**2.39**%	**2.61**%	**1.47**%	**1.08**%	**5.04**%	**4.11**%	**2.46**%	**1.83**%
0.75	-0.05%	**1.51**%	**0.73**%	**0.47**%	**1.13**%	**2.16**%	**1.21**%	**0.81**%
1.25	-2.56%	**0.7**%	**0.15**%	**0.03**%	-2.24%	**0.94**%	**0.22**%	**0.05**%
1.5	-3.37%	**0.42**%	**0.05**%	0%	-3.31%	**0.51**%	**0.05**%	0 %
2	-4.34%	**0.11**%	0%	0%	-4.5%	**0.07**%	0%	0%

time during the production run. As a consequence, before we make any conclusions regarding the superiority of the proposed scheme, in Table 6 the performance of the WSR EWMA chart is compared to the Sign EWMA chart under different *on-to-off-target* process scenarios (δ, I, i, n). In particular, for $(N_h = 150, I = 10, n = 15)$, $\lambda = 0.05$ and $\text{FAP}_0 = 0.1$ the differences Δ defined in (4) between the Sign and the WSR EWMA charts are reported for $i \in \{3, 5, 7, 9\}$, for different shift magnitudes. It can be clearly seen that the results presented in Table 6 are consistent with those in Table 4. In particular, Table 6 shows that, regardless of the time when the shift occurs and even for cases when an assignable cause occurs close to the end of the production run, i.e. before inspections ($i \in \{7, 9\}$ in our case), the WSR EWMA chart performs the better for small to moderate shifts. As a result, for all the investigated process scenarios, we may conclude that the WSR EWMA chart has an overall better performance against its competitors for detecting small to moderate shifts in the process location.

Table 5. Performance comparisons between the WSR EWMA chart with TV limits and the Shewhart WSR chart. *Off-target* process scenario, $(i = 1)$.

$N_h = 150, I = 10, \text{FAP}_0 \approx 0.01$
$(n, C) = \{(10, 49), (15, 88), (20, 134)\}$

		N(0, 1)			$t(8)$	
δ	$n = 10$	$n = 15$	$n = 20$	$n = 10$	$n = 15$	$n = 20$
0.25	**65.17**%	**70.14**%	**73.82**%	**66.22**%	**69.49**%	**69.84**%
0.5	**66.64**%	**27.05**%	**13.87**%	**52.84**%	**20.49**%	**10.13**%
0.75	**18.94**%	**2.65**%	**0.26**%	**12.91**%	**1.54**%	-0.04%
1.25	-0.98%	-0.65%	-0.1%	-0.98%	-0.67%	-0.12%
1.5	-1.54%	-0.18%	-0.01%	-1.27%	-0.31%	-0.02%
2	-0.55%	0%	0%	-0.58%	-0.05%	0%
		$L\left(0, \frac{\sqrt{3}}{\pi}\right)$			$CN(0.05, 2)$	
δ	$n = 10$	$n = 15$	$n = 20$	$n = 10$	$n = 15$	$n = 20$
0.25	**65.17**%	**70.14**%	**73.82**%	**66.22**%	**69.49**%	**69.84**%
0.5	**66.64**%	**27.05**%	**13.87**%	**52.84**%	**20.49**%	**10.13**%
0.75	**18.94**%	**2.65**%	**0.26**%	**12.91**%	**1.54**%	-0.04%
1.25	-0.98%	-0.65%	-0.1%	-0.98%	-0.67%	-0.12%
1.5	-1.54%	-0.18%	-0.01%	-1.27%	-0.31%	-0.02%
2	-0.55%	0%	0%	-0.58%	-0.05%	0%

$N_h = 150, I = 10, \text{FAP}_0 \approx 0.05$
$(n, C) = \{(10, 38), (15, 69), (20, 105)\}$

		N(0, 1)			$t(8)$	
δ	$n = 10$	$n = 15$	$n = 20$	$n = 10$	$n = 15$	$n = 20$
0.25	**0.84**%	**5.72**%	**6.4**%	**3.49**%	**7.38**%	**6.78**%
0.5	**6.86**%	**2.3**%	**0.44**%	**5.44**%	**1.54**%	**0.15**%
0.75	**0.53**%	-0.4%	-0.48%	**0.24**%	-0.42%	-0.41%
1.25	-0.57%	-0.07%	-0.01%	-0.51%	-0.09%	-0.01%
1.5	-0.23%	-0.01%	0%	-0.28%	-0.02%	0%
2	-0.01%	0%	0%	-0.05%	0%	0%
		$L\left(0, \frac{\sqrt{3}}{\pi}\right)$			$CN(0.05, 2)$	
δ	$n = 10$	$n = 15$	$n = 20$	$n = 10$	$n = 15$	$n = 20$
0.25	**3.04**%	**6.35**%	**6.31**%	**1.33**%	**6.78**%	**6.69**%
0.5	**5.13**%	**1.51**%	**0.06**%	**6.12**%	**1.86**%	**0.21**%
0.75	**0.2**%	-0.46%	-0.43%	**0.21**%	-0.5%	-0.44%
1.25	-0.53%	-0.1%	-0.01%	-0.5%	-0.06%	-0.01%
1.5	-0.28%	-0.02%	0%	-0.18%	0%	0%
2	-0.05%	0%	0%	-0.01%	0%	0%

Table 6. Performance comparisons in terms of $\overline{\text{SP}}(i)$ for $i \in \{3, 5, 7, 9\}$ between the Sign and WSR EWMA charts for $(N_h = 150, I = 10)$ with TV limits. *On-to-off-target* process scenario.

$\text{FAP}_0 = 0.1$

	N(0, 1)				$t(8)$			
δ	$i = 3$	$i = 5$	$i = 7$	$i = 9$	$i = 3$	$i = 5$	$i = 7$	$i = 9$
0.25	**14.41**%	**14.56**%	**9.94**%	**0.45**%	**24.73**%	**29.48**%	**25.68**%	**15.91**%
0.5	**6.12**%	**10.09**%	**15.13**%	**11.39**%	**9.28**%	**16.42**%	**26.24**%	**26.47**%
0.75	**2.45**%	**3.59**%	**6.96**%	**7.87**%	**3.51**%	**5.73**%	**11.63**%	**19.09**%
1	**1.01**%	**0.77**%	**1.82**%	**1.24**%	**1.48**%	**1.69**%	**3.57**%	**7.08**%
1.5	-0.59%	-1.85%	-3.29%	-9.69%	-0.41%	-1.75%	-2.81%	-8.63%
	$L\left(0, \frac{\sqrt{3}}{\pi}\right)$				$CN(0.05, 2)$			
δ	$i = 3$	$i = 5$	$i = 7$	$i = 9$	$i = 3$	$i = 5$	$i = 7$	$i = 9$
0.25	**8.74**%	**10.46**%	**7.05**%	**1.11**%	**13.9**%	**15.03**%	**10.2**%	**1.73**%
0.5	**3.17**%	**5.62**%	**8.74**%	**6.97**%	**5.72**%	**9.52**%	**14.55**%	**14.21**%
0.75	**1.16**%	**1.48**%	**3.22**%	**2.27**%	**2.28**%	**3.18**%	**6.46**%	**7.65**%
1	**0.39**%	-0.24%	-0.14%	-2.53%	**0.44**%	-0.19%	-0.1%	-2.42%
1.5	-0.61%	-2.08%	-3.36%	-10.13%	-0.45%	-1.8%	-2.86%	-8.86%

5. Illustrative example

In this Section, we discuss a practical implementation of the WSR EWMA chart under the FHP framework on a real-life dataset related to a filling process of carbonated beverages into cans or polyethylene terephthalate (PET)/glass bottles, where frequent machine changeovers are scheduled to change the soft drink to be filled and the packaging size (see Celano and Chakraborti (2021)). In these processes, the measurement rate of some important quality characteristics is very slow: among them, monitoring the carbon dioxide content of the soft drink filling a bottle/can is worth of attention by practitioners. Usually, only a few inspections can be scheduled between two consecutive changeovers. For the considered production horizon, $I = 10$ inspections have been scheduled. In particular, at each inspection $i \in \{1, 2, \ldots, 10\}$ a sample of $n = 10$ observations of the carbon dioxide content within the soft drink is collected, according to the company's inspection policy. Then, the deviation X from the target value of the carbon dioxide content is calculated. The nominal value of the median deviation is $\theta_0 = 0.095$. It is worth stretching that the distribution of the carbon dioxide content is unknown. Based on past process knowledge, practitioners know that it is symmetric around its median value. The original dataset along with the values of the charting statistic Z_i at each inspection are presented in Table 7. Moreover, setting $\lambda = 0.05$ and $\text{FAP}_0 = 0.1$, we get $K = 1.88$. In Figure 5, the WSR EWMA control chart with time-varying limits (right panel) and asymptotic limits (left panel) are plotted for the $I = 10$ scheduled inspections during the production run. Implementing a control chart with time-varying limits allows process location shifts to be quickly detected. In fact, for the control chart with asymptotic limits, an off-target signal is triggered only at inspection #9. On the other hand, using time-varying limits, the chart triggers a signal at inspection #6. Furthermore, at inspections #4 and #5 the plotted points next to the lower control limit already reveal a process shift leading to a lower amount of carbon dioxide within the carbonated drink to be packaged. A root cause search origi-

Table 7. Example: Observations of carbon dioxide content X_{ij} of $I = 1, \dots 10$ samples having size $n = 10$ and the corresponding values for and the corresponding values for SR_i, Z_i and UCL(i)and LCL(i). Target median $\theta_0 = 0.0905$

	$X_{i,j}$													
i	1	2	3	4	5	6	7	8	9	10	SR_t	Z_i	UCL(i)	LCL(i)
1	0.11	0.14	0.09	0.11	0.09	0.08	0.12	0.08	0.11	0.12	35.00	1.75	1.84	-1.84
2	0.10	0.10	0.11	0.12	0.07	-0.04	-0.04	0.04	-0.05	-0.05	-33.00	-1.65	2.54	-2.54
3	0.07	0.06	0.14	0.06	0.05	0.11	0.05	0.06	0.06	0.08	-31.00	-3.12	3.04	-3.04
4	0.06	0.14	0.03	0.03	0.03	0.10	0.03	0.10	0.02	0.08	-39.00	-1.95	3.43	-3.43
5	0.10	0.10	0.14	0.08	0.08	0.12	0.14	0.05	0.05	-0.01	-5.00	-2.10	3.74	-3.74
6	0.10	0.10	0.04	0.06	0.06	0.12	0.11	0.11	0.05	0.05	-25.00	-3.25	4.00	-4.00
7	0.06	0.06	0.15	0.14	0.14	0.14	0.11	0.11	0.15	0.15	41.00	2.05	4.23	-4.23
8	0.15	0.15	0.15	0.12	0.12	0.14	0.14	0.05	0.05	0.13	37.00	3.80	4.42	-4.42
9	0.12	0.12	0.12	0.12	0.12	0.12	0.12	0.13	0.15	0.15	55.00	2.75	4.59	-4.59
10	0.14	0.15	0.14	0.14	0.14	0.14	0.12	0.12	0.13	0.07	53.00	5.26	4.73	-4.73

nating from the control chart's signal has revealed a problem at the pressure regulator. After eliminating the problem, a second signal is triggered at inspection #9 due to a pressure overcompensation.

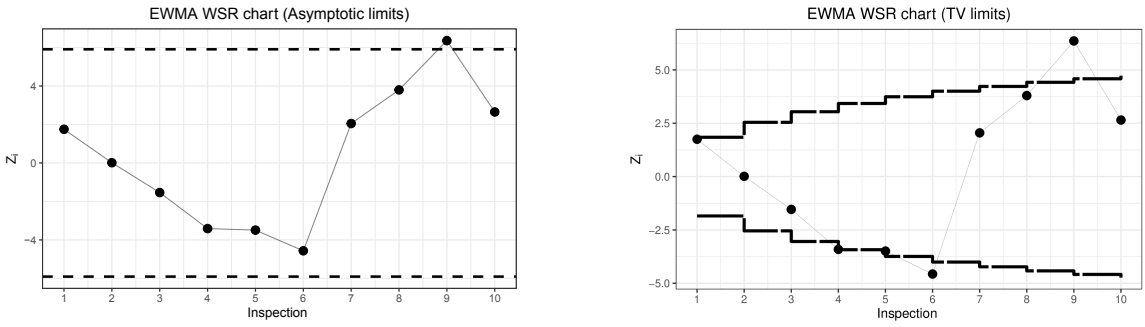

Figure 5. Example: the WSR EWMA chart for the data presented in Table 7 with asymptotic limits (left panel) and time-varying limits (right panel)

6. Conclusions

In this work the performance of an EWMA chart based on the Wilcoxon signed rank statistic has been investigated for monitoring finite horizon processes. Using appropriate metrics of statistical performance and carrying out an extensive numerical analysis, the chart's design parameters have been selected and its off-target performance has been investigated. Additionally, performance comparisons have been discussed among the WSR EWMA, the Sign EWMA and WSR Shewhart charts. The obtained results show that the WSR EWMA chart can be considered as an efficient tool for monitoring small to moderate shifts in the process location regardless of the process scenario being considered. In fact, for on-line process monitoring of a FHP, the WSR EWMA control chart overperforms its competitors for small and medium

shift sizes of the process location.

As a suggested future research directions in the field of distribution-free control charts for monitoring finite horizon production processes, many topics can be suggested. First of all, further research is required on joint monitoring schemes for location and scale. Particular attention should be paid to situations when a target value cannot be defined *a priori* and a reference sample should be considered at the beginning of the production run. An extension to multivariate observations must be carefully investigated as well, because current sensor technologies allow many process parameters to be contemporarily recorded. To boost the control chart's sensitivity, improved adaptive schemes can be taken into account. Finally, it is worth remembering that, currently, there aren't any software packages implementing control charts for the FHP scenario. Efforts in this direction are welcome to bridge the gap between academic research and industrial practice. Open source software like the Shiny package for R can be a good programming environment to develop distribution-free SPM web applications to be shared by quality practitioners within manufacturing companies.

Appendix A

The statistical on-target performance for the WSR EWMA control chart is evaluated through a modified version of the method of Brook and Evans (1972) as discussed by Celano and Castagliola (2018) for the Sign EWMA chart. In particular, the wider control interval $[\mathrm{LCL}(I), \mathrm{UCL}(I)]$ is divided into $2m+1$ subintervals of width $2\rho = \frac{\mathrm{UCL}(I)-\mathrm{LCL}(I)}{2m+1}$. The Markov chain has $S = 2m+3$ states. Note that for the I-th control interval all these states are transient from $s \in \{2, \ldots, 2m+2\}$. Additionally, let H_a, $a \in \{2, \ldots, 2m+2\}$, represents the midpoint of the a-th subinterval. The regions below $\mathrm{LCL}(I)$ (denoted as state $s = 1$) and above $\mathrm{LCL}(I)$ (denoted as state $s = 2m+3$) correspond to the absorbing states at inspection I. On the other hand, due to the fact that for $i < I$ the control interval is tightened due to time-varying limits, some originally transient states $2 \leq s \leq 2m+2$ fall outside the interval and they become absorbing states. Similarly to Celano and Castagliola (2018), a state is considered as absorbing if at the i-th inspection $H_s - \rho < \mathrm{LCL}(i)$ or $H_s + \rho > \mathrm{UCL}(i)$, with $s = \{1, \ldots, S\}$. Finally, the transient probabilities matrix takes the following form:

$$\mathbf{P}(i) = \begin{pmatrix} 1 & 0 & \dots & 0 & 0 \\ 0 & 1 & \dots & 0 & 0 \\ \vdots & \vdots & \dots & \vdots & \vdots \\ p_{(j(i)+1),1} & p_{(j(i)+1),2} & \cdots & p_{(j(i)+1),S-1} & p_{(j(i)+1),S} \\ \vdots & \vdots & \dots & \vdots & \vdots \\ p_{(S-j(i)+1),1} & p_{(S-j(i)+1),2} & \cdots & p_{(S-j(i)+1),S-1} & p_{(S-j(i)+1),S} \\ \vdots & \vdots & \dots & \vdots & \vdots \\ 0 & 0 & \dots & 1 & 0 \\ 0 & 0 & \dots & 0 & 1 \end{pmatrix}$$

where $j(i) = \max[s : H_s - \rho < \text{LCL}(i)]$. If we consider as an example the case where $i = I$, then the transient probabilities matrix is equal to:

$$\mathbf{P}(i) = \begin{pmatrix} 1 & 0 & \dots & 0 & 0 \\ p_{2,1} & p_{2,2} & \cdots & p_{2,S-1} & p_{2,S} \\ \vdots & \vdots & \dots & \vdots & \vdots \\ p_{(S-1),1} & p_{(S-2),2} & \cdots & p_{(S-1),S-1} & p_{(S-1),S} \\ 0 & 0 & \dots & 0 & 1 \end{pmatrix}$$

The transient probabilities $p_{a,b}$ are computed as:

- for $j(i) + 1 > a$ or $S - j(i) < a$:
  $p_{a,b} = 1$ $(a = b)$ or $p_{a,b} = 0$ (otherwise)
- $j(i) + 1 \leq a \leq S - j(i)$:
  $p_{a,b} = \text{P}(H_b - \rho \leq \lambda \text{SR}_i + (1 - \lambda)Z_{i-1} \leq H_b + \rho | Z_{t-1} = H_a)$.

After some simple calculations the above probabilities can be derived as:

$$\begin{aligned} p_{a,b} =& F_{\text{SR}_i^+}\left(\frac{1}{2}\left(\frac{H_b + \rho - (1-\lambda)H_a}{\lambda} + \frac{n(n+1)}{2}\right)\middle| n\right) \\ & - F_{\text{SR}_i^+}\left(\frac{1}{2}\left(\frac{H_b - \rho - (1-\lambda)H_a}{\lambda} + \frac{n(n+1)}{2}\right)\middle| n\right) \end{aligned}$$

where $F_{\text{SR}_i^+}(\dots)$ is the c.d.f. of SR_i^+. Furthermore, let

$$\mathbf{W}(i) = \prod_{t=1}^{i} \mathbf{P}(t)$$

denote the the on-target matrix containing the i-step transition probabilities for $i = \in \{1, 2, \dots, I\}$. Finally, the FAP value, defined as the probability to have a false alarm by the end of the production run, can be derived as:

$$\text{FAP} = \mathbf{q}^{\intercal}\mathbf{W}(I)\mathbf{r}$$

where $\mathbf{q} = (q_{1,1}, \ldots, q_{1,S})^{\intercal}$ is the $(2m+1, 1)$ vector of initial probabilities which is set to $\mathbf{q} = (0, \ldots, 1, \ldots, 0)^{\intercal}$. Moreover, $\mathbf{r}$ denotes a vector with elements $\mathbf{r} = (1, \ldots, 0, \ldots, 1)^{\intercal}$.

Appendix B

In Table 8, we present the off-target performance of the WSR EWMA chart assuming the $\mathrm{N}(0, 1)$ distribution. The *off-target* performance is calculated by means of simulation. Here, we investigate the effect of the number of simulation runs N_{sim} on the accuracy of estimation of the chart's detection capability. We have considered $N_{sim} = \{10^5, 5 \times 10^5, 10^6, 1.5 \times 10^6\}$. For illustration purposes we randomly use $(\lambda, K) = (0.05, 1.88)$ and $n \in \{10, 15\}$. Each column in Table 8 represents a different value of N_{sim} for Monte Carlo simulation. The entries in each table's row show that, neither the $\mathrm{SP}(1, g)$ nor the $\overline{\mathrm{SP}}(1)$ values are significantly affected by N_{sim}, with some minor difference in the fourth decimal place for some cases. As a consequence, the simulation method is a robust approach for determining the chart's off-target performance. For our investigation we have chosen $N_{sim} = 10^6$.

References

Brook, D. and Evans, D.A. An Approach to the Probability Distribution of CUSUM Run Length.Biometrika,1972;59(3):539–549.

Castagliola, P. and Celano, G. and Fichera, S. and Nenes, G. The Variable Sample Size t Control Chart for Monitoring Short Production Runs. The International Journal of Advanced Manufacturing Technology,2013;66(9-12):1353–1366.

Castagliola, P. and Tran, K.P. and Celano, G. and Maravelakis, P.E. The Shewhart Sign Chart with Ties: Performance and Alternatives. Distribution-Free Methods for Statistical Process Monitoring and Control, 2020; Springer International Publishing

Celano, G. and Castagliola, P. and Chakraborti, S. Joint Shewhart Control Charts for Location and Scale Monitoring in Finite Horizon Processes. Computers & Industrial Engineering,2016;101:1427–439

Celano, G. and Chakraborti, S. A distribution-Free Shewhart-type Mann-Whitney Control Chart for Monitoring Finite Horizon Productions. International Journal of Production Research,2021;59(20):6069–6086

Celano, G. and Castagliola, P. An EWMA Sign Control Chart with Varying Control Limits for Finite Horizon Processes. Quality and Reliability Engineering International,2018;34(8):1717–1731

Table 8. Simulated values for $\mathrm{SP}(1,g)$ and $\overline{\mathrm{SP}}(1)$ under the $\mathrm{N}(0,1)$ distribution, for $(\lambda, K = 0.05, 1.88)$ and $n\ in\{10,15\}$. $N_{sim} = \{10^5, 5\times10^5, 10^6, 1.5\times10^6\}$

$n = 10$

	$\delta = 0.5$				$\delta = 75$			
g	10^5	5×10^5	10^6	1.5×10^6	10^5	5×10^5	10^6	1.5×10^6
1	0.3299	0.3304	0.3307	0.3304	0.6027	0.6015	0.6010	0.6015
2	0.6134	0.6129	0.6131	0.6126	0.9014	0.8999	0.8992	0.8994
3	0.7977	0.7957	0.7954	0.7960	0.9803	0.9801	0.9797	0.9801
4	0.8964	0.8976	0.8971	0.8974	0.9964	0.9966	0.9964	0.9965
5	0.9501	0.9501	0.9501	0.9503	0.9995	0.9994	0.9994	0.9994
6	0.9767	0.9766	0.9764	0.9765	0.9999	0.9999	0.9999	0.9999
7	0.9895	0.9890	0.9892	0.9893	1.0000	1.0000	1.0000	1.0000
8	0.9952	0.9950	0.9952	0.9952	1.0000	1.0000	1.0000	1.0000
9	0.9980	0.9978	0.9979	0.9979	1.0000	1.0000	1.0000	1.0000
10	0.9991	0.9990	0.9991	0.9990	1.0000	1.0000	1.0000	1.0000
$\overline{\mathrm{SP}}(1)$	0.8546	0.8544	0.8544	0.8545	0.9480	0.9478	0.9476	0.9477

$n = 15$

	$\delta = 0.5$				$\delta = 75$			
g	10^5	5×10^5	10^6	1.5×10^6	10^5	5×10^5	10^6	1.5×10^6
1	0.4422	0.4445	0.4440	0.4442	0.7717	0.7706	0.7704	0.7707
2	0.7780	0.7801	0.7801	0.7803	0.9800	0.9786	0.9789	0.9788
3	0.9212	0.9222	0.9223	0.9225	0.9986	0.9985	0.9984	0.9986
4	0.9752	0.9747	0.9747	0.9746	0.9999	0.9999	0.9999	0.9999
5	0.9925	0.9923	0.9923	0.9923	1.0000	1.0000	1.0000	1.0000
6	0.9977	0.9976	0.9977	0.9977	1.0000	1.0000	1.0000	1.0000
7	0.9993	0.9994	0.9993	0.9993	1.0000	1.0000	1.0000	1.0000
8	0.9998	0.9998	0.9998	0.9998	1.0000	1.0000	1.0000	1.0000
9	0.9999	1.0000	0.9999	0.9999	1.0000	1.0000	1.0000	1.0000
10	1.0000	1.0000	1.0000	1.0000	1.0000	1.0000	1.0000	1.0000
$\overline{\mathrm{SP}}(1)$	0.9106	0.9111	0.9110	0.9111	0.9750	0.9748	0.9748	0.9748

Celano G, Castagliola P, Chakraborti S, et al. The Performance of the Shewhart Sign Control Chart for Finite Horizon Processes. The International Journal of Advanced Manufacturing Technology. 2016;84(5-8):1497–1512.

Celano G, Chakraborti S,. A Distribution-free Shewhart-type Mann–Whitney Control Chart for Monitoring Finite Horizon Productions. International Journal of Production Research. 2016;59(20):6069–6086.

Celano G, Castagliola P, Chakraborti S, Nenes G. On the Implementation of the Shewhart Sign Control Chart for Low-volume Production. International Journal of Production Research. 2016;54(19):5886–5900.

Chakraborti, S. and Graham, M.A.Nonparametric (Distribution-Free) Control Charts: An Updated Overview and Some Results.Quality Engineering,2019;31(4):523–544

Chakraborti, S. and Celano, G. and Castagliola, P. and Nenes, G.Finite Horizon Process Monitoring. Wiley StatsRef: Statistics Reference Online,2021; John Wiley & Sons, Ltd

Gibbons, J.D. and Chakraborti, S. Nonparametric Statistical Inference,2014;CRC press

Graham M, Chakraborti S, Human S. A Nonparametric Exponentially Weighted Moving Average Signed-Rank Chart for Monitoring Location. Computational Statistics & Data Analysis. 2011;55(8):2490–2503.

Nenes, G. and Tagaras, G. Evaluation of CUSUM Charts for Finite-Horizon Processes. Communications in Statistics—Simulation and Computation,2010;39(3):578–597.

Nenes, G. and Castagliola, P. and Celano, G. and Panagiotidou, S. The Variable Sampling Interval Control Chart for Finite-Horizon Processes. IIE Transactions,2014; 46(10):1050–1065.

Nenes, G. and Castagliola, P. and Celano, G. Economic and Statistical Design of Vp Control Charts for Finite-Horizon Processes. IIE Transactions,2017;49(1):110–125

Nikolaidis, Yiannis and Tagaras, George. New Indices for the Evaluation of the Statistical Properties of Bayesian $\bar{X}$ Control Charts for Short Runs.European Journal of Operational Research,2017;259(1):280–292.

Page E. Continuous Inspection Schemes. Biometrika. 1954;41(1/2):100–115.

Roberts S. Properties of Control Chart Zone Tests. Bell System Technical Journal. 1958;37(1):83–114.

Shewhart W. Statistical Method from the Viewpoint of quality control, graduate school department of agriculture. Washington, DC. 1939;.

Wang, J. and Lee, C.-G. Multistate Bayesian Control Chart Over a Finite Horizon. Operations Research,2015;64(4):949–964. Springer International Publishing

Zimmer, L.S. and Montgomery, D.C and Runger, G.C. Guidelines for the Application of Adaptive Control Charting Schemes. International Journal of Production Research,2000;38(4):1977–1992.